Electron-impact dissociation of CD_3^+ and CH_3^+ ions producing CD_2^+, CH^+, and C^+ fragment ions

E. M. Bahati,* M. Fogle,† C. R. Vane, and M. E. Bannister‡
Physics Division, Oak Ridge National Laboratory, Oak Ridge, Tennessee 37831-6372, USA

R. D. Thomas and V. Zhaunerchyk
Department of Physics, Albanova, Stockholm University, SE106 91 Stockholm, Sweden
(Received 3 March 2009; published 11 May 2009)

Using a crossed electron-ion beams method, we measured absolute cross sections for electron-impact dissociation of the CD_3^+ molecular ions producing CD_2^+ fragment ions and CH_3^+ ions yielding CH^+ and C^+ fragment ions over a collision energy range from a few eV up to 100 eV. The total experimental uncertainties are about 12% at the maximum of the curves of cross sections (peak of the cross section for the CH^+ channel). The obtained results suggest important roles played by predissociation of bound states in the production of both the CH^+ and C^+ fragment ions. Good agreement is found with other results reported for the CH^+ fragment, but some differences are found for the CD_2^+ and C^+ fragments.

DOI: 10.1103/PhysRevA.79.052703 PACS number(s): 34.80.Ht, 34.80.Gs

I. INTRODUCTION

Collision processes play pivotal roles in the dynamics of such diverse areas as laboratory plasmas, thermonuclear fusion, and astrophysics. For example, in fusion energy technology, the plasma-facing walls may interact with plasma particles (neutrals and ions) and eroded impurities of the wall material may then enter the plasma and strongly influence its properties. Carbon is the most abundant material used in these walls and the methyl radical, CH_3, and the acetylene molecule, C_2H_2, as well as their ions, are expected to be the abundant sputtered fragments [1]. It is therefore clear that high-quality experimental measurements of the collision properties of these neutral and ionic species are needed in studies of edge fusion plasma. Furthermore, high-quality data are needed as benchmarks to test and validate theoretical models, when available, and provide information for diagnosing plasma media.

Both the methyl radical, CH_3, and its cation, CH_3^+, are observed in many other plasma media and have long been recognized as being among the most fundamental reactive species in chemical reactions occurring in those media [2–8]. CH_3 is a particularly important intermediate product in reactions leading to the production of hydrocarbons, e.g., in the synthesis of petroleum derivatives in laboratories or in the chemical kinetics driven by cosmic rays in the interstellar medium. In addition, its ion, CH_3^+, is able to capture electrons and functional groups from a variety of neutral organic molecules. It even reacts with saturated hydrocarbons to produce more stable compounds. Because of their nature and paramount importance, these two molecules (neutral and ionic) have been the subject of many theoretical and experimental studies. However, laboratory investigations are difficult as a consequence of (a) the inherently more complex structure of molecular species relative to atoms in general and (b) the extremely reactive nature of CH_3 and, in particular, CH_3^+ [7–9]. Indeed, despite the apparent simplicity of these two compounds, it has been difficult to obtain accurate laboratory measurements of their molecular parameters since, as radicals, they recombine very easily with other particles in a gas, i.e., with residual gas molecules. This feature also applies to other hydrocarbon ions of the series CH_n^+ and $C_2H_m^+$ ($n=2-4$ and $m=1-7$) which are equally important in organic chemical kinetics [3].

Several studies exploring the structural, reactive, and spectroscopic properties of hydrocarbons have been carried out [2–8,10–16] but results remain sparse. In 2000 and 2002, collections of data on interactions of hydrocarbons with hydrogen and with electrons were made available by Alman and Ruzic [17] and by Janev and Reiter [18,19] for the CH_n and the C_mH_n families and their ionized homologs, respectively. Since then, new investigations based either on the improved understanding of the physical mechanisms governing those processes or on entirely new experimental methods have been performed. Most of these studies explore the fragmentation of the molecules via the dissociative recombination (DR) process. DR involves the efficient capture of a low energy electron (≤ 1 eV) by the molecular ion which then stabilizes its excess energy by dissociating into neutral fragments. Two recent reviews of measurements of DR of hydrocarbon ions at ion storage rings have been reported by Viggiano *et al.* [21] and by Mitchell *et al.* [22]. Only a few studies relate to the dissociative excitation (DE) and the dissociative ionization (DI) processes, which differ from DR in that charged fragments are produced in the reaction and are therefore more efficient at higher electron energies (≥ 10 eV), but these studies have been mostly limited to the detection of light fragment ions from the reaction [9,23–27].

In the present paper, we report on absolute cross section measurements for the formation of the CD_2^+ fragment ions from dissociation of the CD_3^+ molecular ion and CH^+ and C^+ fragment ions from CH_3^+ through impact with electrons of energy ranging from 5 up to about 100 eV. The CD_3^+ isotopomer is used for the CH_2^+-CH_3^+ fragment channel in order

*Present address: American Magnetics, Oak Ridge, TN 37830.
†Present address: Department of Physics, Auburn University, Auburn, AL 36849.
‡bannisterme@ornl.gov

TABLE I. Energies for electron-impact dissociation channels of CH_3^+ ions producing CH_2^+, CH^+, and C^+ fragment ions. Vertical transition threshold energies E_{th} are taken from Ref. [18] where available and are given in eV for CH_3^+ ions in the $v=0$ ground state. The dissociation limit energies D_0 are estimated from dissociative recombination measurements in Ref. [28] and ionization energies of neutral fragments given in Ref. [29]. The KERs are from Ref. [18]. Resonant ion pair formation processes are not included; see text for an explanation.

Products	E_{th} (eV)	D_0 (eV)	KER (eV)
	Dissociative excitation		
$CH_2^+ + H$	7.03	5.40	1.62
$CH^+ + H_2$	7.22	5.44	1.67
$CH^+ + 2H$		9.94	
$C^+ + H_2 + H$	12.65	9.66	2.92
$C^+ + 3H$		14.16	
	Dissociative ionization		
$CH_2^+ + H^+$	30.81	19.00	11.78
$CH^+ + H_2^+$		20.87	
$CH^+ + H^+ + H$	35.94	23.54	11.78
$C^+ + H^+ + H_2$	35.09	23.26	11.78
$C^+ + H_2^+ + H$		25.09	
$C^+ + H^+ + 2H$		27.76	

to reduce the background count rate for fragment ions by moving the primary ion beam farther from the detector (see Sec. II for experimental details). Some of the possible reaction channels through which CH_2^+, CH^+, and C^+ fragment ions can be produced from CH_3^+ are given in Table I. D_0 corresponds to the dissociation energy limit. For a given reaction channel, D_0 is estimated using the energy released in the production of ground-state fragments from dissociative recombination of CH_3^+ ion [28] and the ionization potential energies of C, CH, CH_2, H, and H_2 neutral fragments [29]. In contrast, E_{th} corresponds to a threshold energy for a vertical transition from the CH_3^+ ground state to the appropriate dissociative state for the given final products (also in their ground states); the values of E_{th} are averaged over the Franck-Condon region of the vibrational ground state of CH_3^+ and are from the work of Janev and Reiter [18,19]. Resonant ion pair (RIP) formation also produces ion fragments, but for the energy range of the present measurements, the contribution of this process is expected to be negligible [30–32].

Dissociative excitation proceeds by two pathways. Direct dissociative excitation (DDE) involves a Frank-Condon transition from the ground state of the molecular ion directly to a dissociative excited state or a predissociative state, i.e., an excited bound state coupled to a dissociative state. Notice, however, that the predissociation lifetime depends on the vibrational and rotational state of the ion. At low collision energy, another collision process, resonant dissociative excitation (RDE), can also contribute to the measured cross section. This process, also known as capture-autoionization dissociation (CAD), involves the capture of the incident electron into a doubly excited dissociative Rydberg state of the neutral molecule which then subsequently decays by ejecting an electron and dissociating. This process leads to the same reaction products as the DDE process but with smaller threshold energies down to the dissociation limit energy. Hereafter we refer to the DDE and RDE processes together as simply DE.

Dissociative ionization proceeds through a direct process similar to the DDE process but results in the production of two or more charged fragments and the ejection of one or more electrons.

There has been no data reported in studying the heavy ion fragments from the DE and DI reactions of CH_3^+ or CD_3^+. To date, only some preliminary results have been presented at conferences [27,33].

The content of this paper is organized as follows: the experimental method and the apparatus used are briefly described in Sec. II. Results are presented and discussed in Sec. III. The summary and concluding remarks are given in Sec. IV. We note that all of the pathways through which CD_2^+, CH^+, and C^+ fragments ions can be produced from dissociation of CD_3^+ and CH_3^+ by impact of electrons cannot be resolved in the present study. Hence, the measurements reported here represent the contributions summed over all of the possible reaction channels.

II. EXPERIMENT

A. Ion and electron beams

A schematic view of the apparatus used in the present study is shown in Fig. 1. A full description has previously been reported elsewhere [23,34–38] and only a brief summary is given here. The parent ions are produced in the ORNL Caprice electron cyclotron resonance (ECR) ion source [39] fed by methane gas (CH_4 or CD_4) and then extracted and accelerated to 10 keV. The source is typically operated with 1–2 W of microwave power and a gas pressure of approximately $(4-8)\times10^{-7}$ Torr in the ECR region. This typically gives 30–50 μA CD_3^+-CH_3^+ ion beam current after leaving the magnetic mass selector. The beam is then transported with electrostatic and magnetic optics and directed into the collision chamber where it interacts at 90° with a magnetically confined electron beam [40,41]. Products of the interaction are separated from the primary ion beam by means of a magnetic analyzer and directed onto either a channel electron multiplier (CEM) detector or a discrete dynode detector. Initial measurements performed with the CEM were limited to total count rates less than 6×10^4 s^{-1} to avoid signal loss; the discrete dynode detector permits total count rates up to 1×10^6 s^{-1} and has a larger acceptance for the fragment ions. Typical background count rates on the discrete dynode detector, normalized to the primary ion beam current, are 3.2×10^4, 1.1×10^4, and 2.1×10^3 s^{-1} nA^{-1} for the CD_2^+, CH^+, and C^+ fragment ion channels, respectively. The primary ions are collected in a Faraday cup, with typical currents of 30–90 nA.

Special care is taken to eliminate nitrogen from the feeding gas line of the ECR ion source since NH^+ ions, which have mass $m=15$ and electric charge $q=1$, would contami-

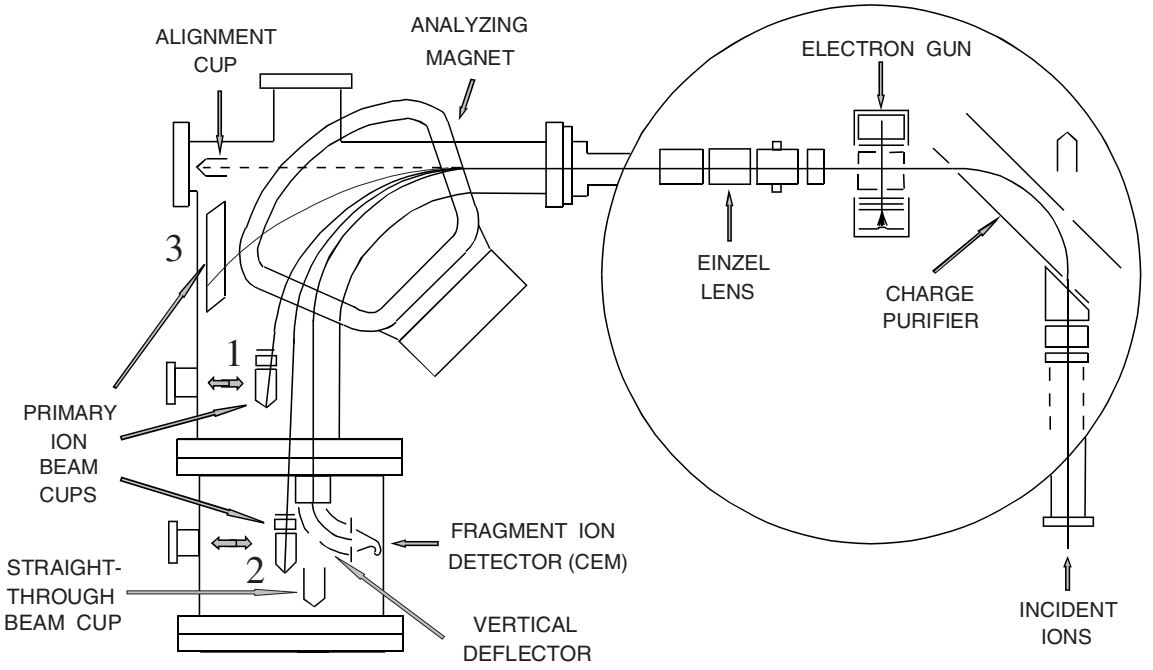

FIG. 1. Electron-ion crossed-beams experimental apparatus. See text for an explanation. The fragment ion detector and vertical deflector are rotated 90° to the plane of the figure.

nate the ion beam. Furthermore, the methane used as the working gas is not 100% pure and may contain some impurities. Hence, contamination from $^{13}CH_2^+$ ions should be considered since, like NH^+, they have the same m/q ratio as the CH_3^+ target ion. In our previous study of the CH_2^+ ion fragmentation [42] we estimated the contribution of N^+ and $^{13}CH^+$ to be less than 6%, considering both nitrogen contamination of the source and the natural abundance of ^{13}C. In the present study, we expect a similar contribution, or even less, for the same reasons. Similarly, contamination from H_2O^+ must also be minimized since those ions have the same m/q ratio as CD_3^+. Analyzed ion spectra extracted from the CD_4 plasma showed a contamination of less than 5% for the CD_3^+ ion beam, as indicated by the population of OH^+ ions.

Though operating at such a minimal microwave power level as 1 W, the ECR source may produce the CD_3^+ and CH_3^+ ions distributed over vibrationally, rotationally, and/or electronically excited states. However, the current experimental construction does not allow us to estimate the fractional abundances of the excited states. Therefore, the measured signal likely contains contributions from these excited states.

B. Diagnostics

It is well known that in an experimental investigation involving a dissociation process, the major obstacle is the high background rate arising from dissociation on residual gas molecules, primarily H_2. Thus, in the case where a very low ratio of signal to background is recorded, the experiment may become difficult to achieve or too time consuming. Furthermore, as dissociation fragments may gain additional kinetic energy from reaction, they could have angular and energy distributions in the laboratory frame which are significantly wider than the acceptance of the detector. This leads to an artificial reduction in the number of detected particles. The maximum projected horizontal displacement due to the energy dispersion of the fragment ions by the analyzing magnet is given by the following relationship [23]:

$$\Delta x_{\max} = 4r_0\left(\frac{\Delta E}{E_i}\frac{M-m}{m}\right)^{1/2}, \tag{1}$$

where ΔE, r_0, E_i, M, and m, are the kinetic energy release (KER) of the reaction, bending radius of the analyzing magnet, the energy and mass of the parent ion, and the mass of the ionic fragment, respectively. Figures 2(a) and 2(b) show the apparent cross section at 100 eV as a function of the analyzing magnetic field measured with the CEM detector. From these data we estimate the maximum displacement of fragment ions from the center of our 5 mm radius CEM detector to be approximately 4.7 mm for the CH^+ channel and 6.2 mm for the C^+ channel. Using Eq. (1), we deduce the upper limit of the corresponding KERs, 2.2 and 2.4 eV for the CH^+ and C^+ channels, respectively. Notice however, these numbers are average values since the CH^+ and C^+ fragment ions are produced through different reaction channels at 100 eV, each of which has its own maximum KER, but our experiment cannot differentiate between them. From the data plotted in Fig. 2(a) we conclude that the size of the ion beam for the CH^+ channel is comparable to the acceptance of the CEM detector, i.e., the total collection of the signal is

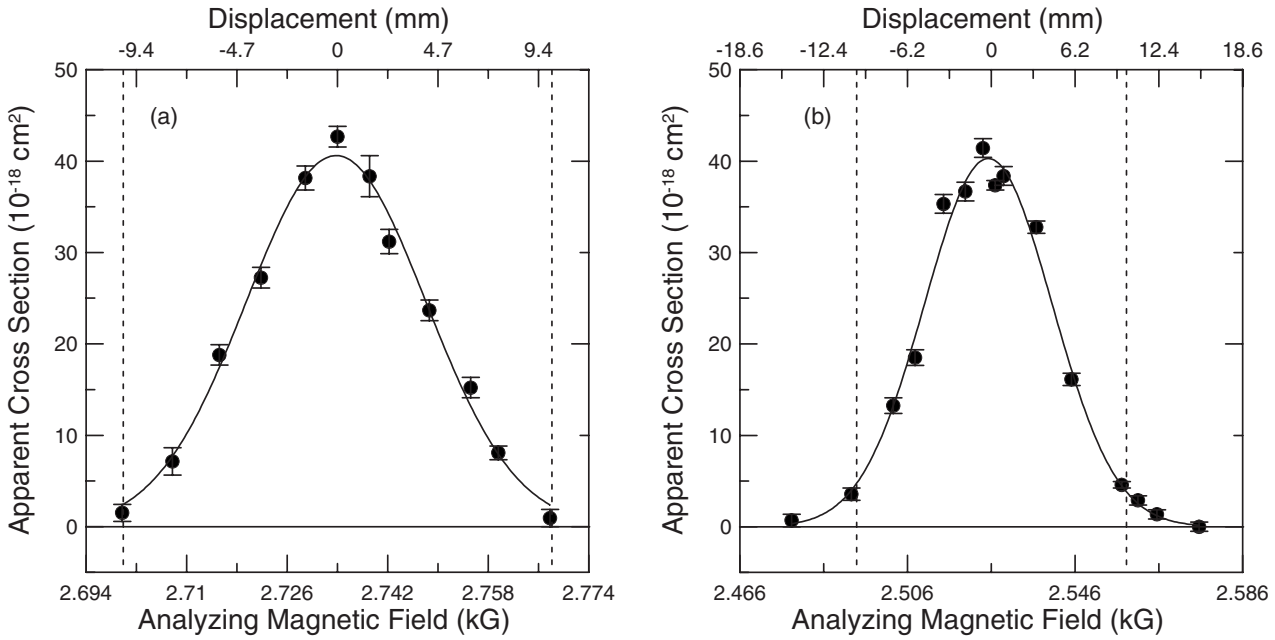

FIG. 2. Apparent cross sections versus analyzer magnetic field measured at incident electron energy of 100 eV. The upper abscissa indicates the displacement of the signal (a) CH^+ and (b) C^+ fragments from the center of the detector by the analyzing field. The dashed vertical lines indicate the limits of our 5 mm radius detector. Solid curves represent the best fit to the data.

achieved in the plane of dispersion at the central value, B_0, of the analyzer magnetic field. On the other hand, from the data plotted in Fig. 2(b), the dispersion of the C^+ ions is greater than the CEM detector, i.e., the total ion signal is not collected at B_0. For a given interaction energy, we correct our measurements by adding to the cross section measured at position B_0 measurements taken at $B_0 \pm \Delta B$, where ΔB is the field needed to move the ion beam by one detector width. The portion of the signal missing the detector for field B_0 represents approximately 3% of the total signal. It is worth pointing out that the measurements obtained using the discrete dynode detector with a bigger acceptance are consistent with the CEM results determined by this summation. Finally, changing the voltage applied on the 90° electrostatic cylindrical analyzer, which directs the fragments into the CEM detector, by several hundred volts on either side of the nominal values used for taking the present data gives a constant signal, indicating that 100% of the ions are detected in the direction perpendicular to the dispersion plane for both CH^+ and C^+ channels. The CD_2^+ fragment channel measurements were performed only using the larger discrete dynode detector and, hence, no plot of apparent cross section as a function of analyzing magnetic field is shown.

C. Cross sections and uncertainties

The absolute cross section, σ, at interaction energy, E, is determined [43] from the measured quantities by the following relationship:

$$\sigma(E) = \frac{R}{I_i I_e} \frac{qe^2 v_i v_e}{\sqrt{v_i^2 + v_e^2}} \frac{F}{\epsilon}, \tag{2}$$

where R is the fragment signal rate, I_i and I_e are, respectively, the incident ion and electron currents, qe is the charge of the incident ions, v_i and v_e are the incident ion and electron velocities, F is the form factor that is determined from the two beam profiles as described below, and ϵ is the fragment ion detection efficiency.

The overlap of the ion and electron beams in the direction perpendicular to both beams (vertical direction) was measured at each interaction energy with a slit probe moving through the center of the interaction region. Current profiles of the ion and electrons, $I_i(z)$ and $I_e(z)$, were measured independently and numerical integration yielded the form factor F needed for determination of absolute cross sections,

$$F = \frac{\int I_e(z)dz \int I_i(z)dz}{\int I_e(z) I_i(z) dz}. \tag{3}$$

The evaluation of the absolute uncertainties on the parameters in Eq. (2) has been performed in our previous studies [34,36]. Despite recent modifications of the apparatus [23], these evaluations remain pertinent. The systematic absolute uncertainties at a 90% confidence level associated with the measurement of the quantities in Eq. (2) are listed in Table II. The major contributions to the total absolute uncertainty are the efficiency of the product ion detection, the collection and transmission of product ions to the detector, and the measurement of the form factor, which may change during a measurement. The quadrature sum of those components gives a $\pm 8.5\%$ contribution to the uncertainty of the measured cross section.

For measurements at lower collision energies, much time is needed to achieve a reasonable statistical uncertainty, more than 10 h per single data point. In these cases, we observe

TABLE II. Absolute systematic uncertainties at a high confidence level equivalent to 90% confidence for statistical uncertainties.

Source	Uncertainty (%)
Fragment ion detection	±5
Signal transmission	±5
Form factor	±4
Ion current	±3
Electron current	±2
Ion velocity	±1
Electron velocity	±1
Quadrature sum	±8.5

small changes in the form factor between the beginning and the end of the run corresponding to a ±2% variation.

For each single measurement, all the above mentioned contributions are combined with the total relative uncertainty to yield the absolute total uncertainty, shown in Table III, at a level equivalent to a 90% confidence level for statistical uncertainties.

III. RESULTS

Absolute measurements of the cross sections for the production of CD_2^+, CH^+, and C^+ fragment ions from electron-impact dissociation of the CD_3^+ and CH_3^+ molecular ions are made over a collision energy range from threshold up to 100 eV. The results are listed in Table III together with the collision energies and the corresponding relative and absolute total expanded uncertainties. The measured cross sections for the CD_2^+, CH^+, and C^+ channels are also presented as filled circles in Figs. 3–5, respectively, with the error bars corresponding to the absolute total expanded uncertainties. The cross section data reported represent the sum of all processes through which CD_2^+, CH^+, and C^+ fragment ions can be produced from dissociation of CD_3^+ and CH_3^+ by electron impact. Owing to limitations of the experimental technique and the lack of potential energy surfaces reported for CH_3^+ and CH_3, we cannot perform a more complete quantitative analysis. Nonetheless, there are empirical predictions for some of the dissociation channels of the CH_3^+ molecular ion as well as preliminary measurements [27,33] on dissociation of CD_3^+ which are used for comparison with the present results.

A. CD_2^+ fragments

The measured cross sections for the production of CD_2^+ fragment ions shown in Fig. 3 exhibit two distinct sections divided by the threshold for dissociative ionization. Below this threshold, only dissociative excitation contributes to the cross section. The lowest energy measurements suggest a DE threshold of about 5 eV, consistent with the dissociation limit energy D_0 given in Table I. The cross section rises quickly to almost its maximum value by an energy equivalent to the vertical transition threshold, E_{th}, and then exhibits a broad peak. Two possible explanations exist for this behavior: first, the RDE process contributes significant dissociation above D_0 or, second, excited states of the CD_3^+ target ion effectively lower the dissociation threshold. The $1\ ^3A''$ and $1\ ^3A'$ metastable electronic states lie 3.56 and 3.86 eV above the ground state, respectively [44]. The vertical transition threshold for these states would be less than 3.5 eV; this is not

TABLE III. Absolute total cross sections of electron-impact dissociation of CD_3^+ and CH_3^+ ions yielding CD_2^+, CH^+, and C^+ fragments. The relative uncertainties are at the one standard deviation level; the total expanded uncertainties given in parenthesis are at a high confidence level equivalent to 90% confidence for relative uncertainties.

	Cross section (10^{-18} cm^2)		
Energy (eV)	CD_2^+	CH^+	C^+
5.4	20.0 ± 12.9(25.9)		
6.2		−2.3 ± 7.2(14.3)	
6.8	48.1 ± 11.0(22.4)		
7.7		17.1 ± 5.9(12.0)	
9.3			3.9 ± 1.5(3.1)
9.4	52.6 ± 12.4(25.3)		
9.5		16.8 ± 4.3(8.7)	
11.6		20.4 ± 4.1(8.4)	
12.0	40.3 ± 5.7(11.9)		
12.4			8.7 ± 4.1(8.3)
14.1		39.0 ± 3.3(7.9)	9.1 ± 1.1(2.3)
14.4	53.5 ± 7.4(15.4)		
16.3		40.6 ± 6.0(12.8)	
19.0			19.6 ± 0.7(2.5)
19.3	33.9 ± 7.8(15.8)	54.0 ± 1.6(6.6)	
23.8		46.6 ± 1.5(5.7)	
23.8			23.3 ± 1.3(3.5)
24.2	33.1 ± 4.7(9.9)		
28.8			23.6 ± 0.7(2.8)
28.9	35.2 ± 3.8(8.1)		
29.3		38.1 ± 2.0(5.7)	
38.8	44.2 ± 3.3(7.6)		
39.0			24.8 ± 0.6(2.9)
39.1		45.7 ± 1.2(5.4)	
48.8	49.8 ± 3.0(7.4)		
58.5	50.8 ± 1.8(5.6)		
59.3		53.5 ± 1.2(6.1)	
60.0			27.2 ± 0.7(3.2)
67.4			26.5 ± 0.3(3.3)
68.8	54.5 ± 2.3(6.5)		
77.5	58.2 ± 1.7(6.0)		
78.8		54.9 ± 1.5(6.6)	
79.6			27.6 ± 0.7(3.0)
97.1		55.3 ± 0.5(6.0)	
97.3	51.2 ± 1.4(5.2)		
99.6			27.2 ± 0.8(3.0)

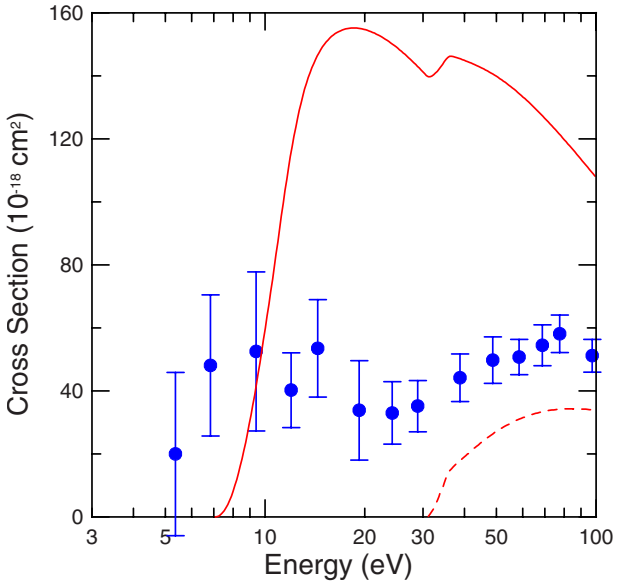

FIG. 3. (Color online) Absolute cross sections versus interaction energy for electron-impact dissociation of CD_3^+ producing CD_2^+ fragment ions. Error bars correspond to absolute total expanded uncertainties. The solid line represents the sum of DE and DI obtained from fitting functions given in Refs. [18,19] and the parameters given in Ref. [20]; the dashed line represents the DI contribution only.

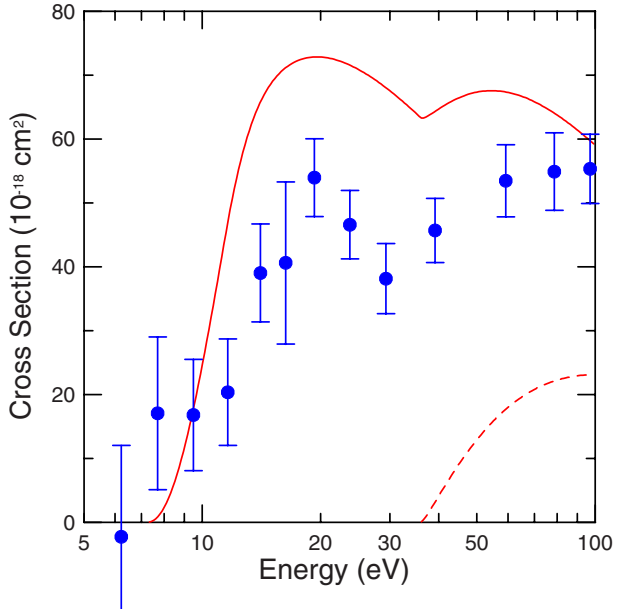

FIG. 4. (Color online) Absolute cross sections versus interaction energy for electron-impact dissociation of CH_3^+ producing CH^+ fragment ions. Error bars correspond to absolute total expanded uncertainties. The solid line represents the sum of DE and DI obtained from fitting functions given in Refs. [18,19] and the parameters given in Ref. [20]; the dashed line represents the DI contribution only.

consistent with the observed threshold behavior. However, ions in higher vibrational levels of the CD_3^+ ground electronic state could effectively lower the vertical transition threshold by at least 2 eV. The threshold behavior of the cross section for production of CD_2^+ fragments will be addressed again after presenting the dissociation measurements for the CH^+ and C^+ channels.

The CD_3^+ ion is a planar molecule [5] and has two bound electronic states that lie above the dissociation limit: $^1E''$ at 6.46 eV and $^1A_2''$ at 17.4 eV above the ground state [45]. Excitations to these allowed states, followed by predissociation through coupled repulsive states, can enhance the DE cross sections. The sharp rise from the observed threshold may be due in part to contributions from excitation to the $^1E''$ state; no obvious enhancement to the cross section from excitations to the $^1A_2''$ state is seen.

The measured cross sections increase for energies above the DI threshold, reaching values over 50×10^{-18} cm^2 for $E\geq50$ eV. The semiempirical predictions of Janev and Reiter [18,19] are also shown in Fig. 3 for comparison. The solid line represents a sum of their predictions for the DDE and DI processes; the dashed line represents predictions for DI only. Although their DI predictions are in good agreement with the experiment, the DDE predictions clearly overestimate the cross section by a factor of almost 3. They provided no predictions for the RDE contribution that may be present just above threshold.

B. CH^+ fragments

The structure of the cross sections we show in Fig. 4 is similar to that observed in our previous measurements on dissociation of DCO^+ by electron-impact producing the CO^+ fragment [38]: a curve with three distinct sections. Rising from a threshold of $\approx7\pm1$ eV, the CH^+ production cross section peaks at about 20 eV before decreasing and then smoothly rising again above 30 eV.

The first section, which ranges from the observed threshold up to around 12 eV, is characterized by small magnitudes for the measured cross sections, the maximum being approximately 17×10^{-18} cm^2. This small cross section at the vertical transition threshold E_{th} indicates that the contribution of both excited states in the CH_3^+ target ions and the RDE process are minimal for this channel, as is any contribution from predissociation through the $^1E''$ state.

Above 12 eV, another rise of the DE cross section coincides with the opening of the $CH^+ + 2H$ channel. At slightly higher energies, a peak appears in the DE cross section, rising to a value of about 54×10^{-18} cm^2 near 20 eV. The sharpness of the peak suggests excitation to a single bound state, namely, the $^1A_2''$ state, followed by predissociation.

The third region ranges from around 30 to 100 eV. The sudden change in slope of the cross section curve observed at the beginning of this region indicates the opening of the first DI channel. As previously mentioned, our experiment cannot separate the contribution of this individual process to the measured signal. The sum of the DE and DI contributions then rises smoothly to a broad peak of about 54×10^{-18} cm^2.

The semiempirical predictions of Janev and Reiter [18,19] for the production of CH^+ fragment ions are also shown in Fig. 4. The solid curve represents the sum of their DE and DI predictions; the dashed curve represents the DI contribution

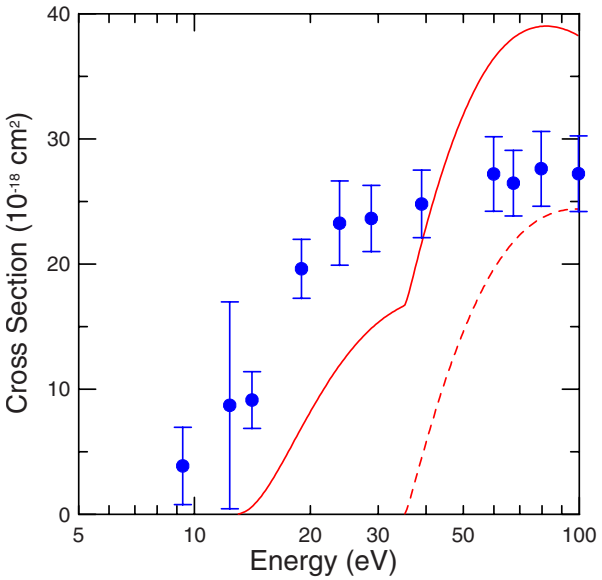

FIG. 5. (Color online) Absolute cross sections versus interaction energy for electron-impact dissociation of CH_3^+ producing C^+ fragment ions. Error bars correspond to absolute total expanded uncertainties. The solid line represents the sum of DE and DI obtained from fitting functions given in Refs. [18,19] and the parameters given in Ref. [20]; the dashed line represents the DI contribution only.

only. As was the case for the CD_2^+ fragments, their DI predictions are in good agreement with the experimental data. However, their predictions for DE, using only the DDE portion and omitting any RDE contribution, exceed the measured cross sections by about 30%. Their formulation does not account for the contribution of excitations to bound excited states followed by predissociation, such as the contribution of the $^1A_2''$ state evident for this channel.

C. C^+ fragments

The energy-dependent cross sections for the production of C^+ fragments are shown in Fig. 5 and, unlike the data observed for the production of CD_2^+ and CH^+, do not exhibit any noticeable structure. The cross section is not zero below the predicted vertical transition threshold energy of the first DE process, 12.65 eV (see Table I). The observed threshold, $\approx 9 \pm 1$ eV, is obtained by extrapolation of data below 14 eV. Nevertheless, the observed threshold energy is comparable to the dissociation energy limit of this channel. This may indicate that, as for the CD_2^+ channel, in the threshold region, C^+ is produced either through RDE mechanisms involving Rydberg states of CH_3^{**} or vertical transitions to repulsive states from higher vibrational levels of the ground state.

The cross section is essentially featureless over the range of the present measurements, with only a slight inflection that is probably associated with the opening of the second DE channel, namely, $C^+ + 3H$, with an expected vertical transition threshold of about 16 ± 1 eV, assuming a similar KER as for the lower DE channel (see Table I). In addition, one cannot rule out a small contribution from excitation to the $^1A_2''$ bound state at 17.4 eV followed by predissociation. A slight increase in the dissociation cross section is observed above the DI thresholds, although no clear onset of these contributions is seen in the measurements.

Figure 5 also shows the semiempirical predictions of Janev and Reiter [18,19] for the production of C^+ fragment ions. The solid curve represents the sum of their DE and DI predictions; the dashed curve represents the DI contribution only. In contrast to the data for the other two fragment channels, their DI predictions seem to overestimate the experimental data. Also, their predictions for DE, using only the DDE portion and omitting any RDE contribution, underestimate the measured cross sections by about 40%.

D. Summary

To address the issue of excited states in the CD_3^+ and CH_3^+ target ion beams, consider the low energy measurements for each of the three heavy fragment channels investigated. None of the three showed any dissociation at 3.5 eV below the vertical transition thresholds, indicating the lack of electronic excited states in the target ions. The threshold behavior of the CH^+ fragment channel is consistent with onset of dissociation through vertical transitions to repulsive states, with minimal contribution from vibrationally excited states. Since the same target ion beam was used for the C^+ fragment channel measurements, one can deduce that those measurements also lack significant contributions from vibrationally excited CH_3^+ ions. However, as to whether there are contributions from vibrationally excited ions to the CD_2^+ channel cross sections is still unanswered. Other possible sources of the significant cross section below the vertical transition threshold for this channel are excitations to the $^1E''$ bound excited state followed by predissociation and the RDE process. Dissociative recombination measurements [28] exhibited two resonance features, one near 2 eV that is below the DE threshold for all the channels in the present study and another around 12 eV that is a few eV wide. This latter peak due to resonant capture could contribute to RDE of CH_3^+ and CD_3^+ if an electron is ejected following the capture, but no clear evidence of this is seen in any of the three measured channels. Therefore, it is likely that excitation and predissociation through the $^1A_2''$ bound state at 17.4 eV give rise to the observed peak in the DE cross section for CH^+ fragment production. Small contributions of this excited state to the CD_2^+ and C^+ channels cannot be ruled out. Excitation and predissociation through the $^1E''$ state may contribute to the near-threshold dissociation of CD_2^+.

The kinetic energies of release determined from Figs. 2(a) and 2(b), 2.2 eV for the CH^+ channel and 2.4 eV for C^+, are close to the values given by Janev and Reiter [18,19] for the direct dissociative excitation process, but much less than the 11.78 eV value they give for KERs of the dissociative ionization process. At an interaction energy of 100 eV, one would expect the measured dissociation cross sections to be dominated by DI since the DE thresholds are in the 5–15 eV range. The mechanism of excitation to a bound excited state followed by predissociation may also make significant contribution to DI while yielding a much lower KER, but sepa-

rate measurements of the DI process alone would be required to substantiate this hypothesis. Such measurements are currently beyond the capabilities of the present apparatus.

It is worth mentioning that measurements on electron-impact dissociation of CD_n^+ were carried out at Louvain-la-Neuve and preliminary results for $n=3$ and $n=4$ presented at two conferences [27,33]. A comparison with the present results yields good agreement for the CH^+ channel, including the peak in the DE cross section here attributed to excitation to the $^1A_2''$ bound state at 17.4 eV followed by predissociation. The overall agreement for the C^+ channel is fair. The shape and magnitude of their results for CD_2^+ channel differs greatly from the present results.

IV. CONCLUSIONS

Cross sections for the formation of CD_2^+ fragments from the dissociation of CD_3^+ molecular ions and formation of CH^+ and C^+ fragments from CH_3^+ ions after collision with an electron have been measured for interaction energies ranging between a few eV up to 100 eV using a crossed electron-ion beams method. The obtained results are compared to other available data from empirical predictions [18,19] and from electron-impact dissociation of CD_3^+ [27]. For the formation of CH^+ fragment, good agreement is found between the present cross sections and semiempirical fits of Janev and Reiter [18,19], as well as with measurements reported on CD_3^+ [27]. However, such good agreement is not observed for the production of the CD_2^+ and C^+ fragments. Data obtained for the CH^+ channel suggest an important role played by predissociation of bound states. Resonant dissociative excitation plays at most only a minor role in dissociation leading to the CH^+ and C^+ fragments. Our analysis and any firmer conclusions that could be drawn are however hampered by the lack of potential energy surfaces for CH_3^+ and CD_3^+ . Future measurements on the dissociation of CH_3^+ will focus on the contributions of rovibrationally excited ions by reducing their population in the target ion beam by utilizing colder sources of ions and by storing the ions for times long enough for radiative relaxation.

ACKNOWLEDGMENTS

This research was supported in part by the Office of Fusion Energy Sciences and the Office of Basic Energy Sciences of the U.S. Department of Energy under Contract No. DE-AC05-00OR22725 with UT-Battelle, LLC. Two of the authors (E.M.B. and M.F.) gratefully acknowledge support from the ORNL Postdoctoral Research Associates Program administered jointly by the Oak Ridge Institute for Science and Education and Oak Ridge National Laboratory. R.D.T. acknowledges the support from the IHP program of the European Community (EC) under Contract No. HPRN-CT-2000-00142. We wish to thank A. C. H. Smith, P. Krstić, and P. Maskens for insightful discussions.

[1] E. Salonen, K. Nordlund, J. Keinonen, and C. H. Wu, Contrib. Plasma Phys. **42**, 458 (2002).
[2] G. D. Stancu, J. Röpcke, and P. B. Davies, J. Chem. Phys. **122**, 014306 (2005).
[3] H. G. Yu and T. J. Sears, J. Chem. Phys. **117**, 666 (2002).
[4] H. Feuchtgruber, F. P. Helmich, E. F. Van Dishoeck, and C. M. Wright, Astrophys. J. **535**, L111 (2000).
[5] M. W. Crofton, M. F. Jagod, B. D. Rehfuss, W. A. Kreiner, and T. Oka, J. Chem. Phys. **88**, 666 (1988).
[6] X. Liu, R. L. Gross, and A. G. Suits, Science **294**, 2527 (2001).
[7] D. S. Marynick and D. A. Dixon, Proc. Natl. Acad. Sci. U.S.A. **74**, 410 (1977).
[8] M. W. Crofton, W. A. Kreiner, M. F. Jagod, B. D. Rehfuss, and T. Oka, J. Chem. Phys. **83**, 3702 (1985).
[9] D. S. Belić, J. J. Jureta, H. Cherkani, and P. Defrance, BPU-5 Fifth General Conference of the Balkan Physical Union, Vrnjacka Banja, Serbia and Montenegro, 25–29 August 2003 (unpublished), p. 317.
[10] S. Hayakawa, B. Feng, and R. G. Cooks, Int. J. Mass Spectrom. Ion Process. **167**, 525 (1997).
[11] W. A. Chupka and C. Lifshitz, J. Chem. Phys. **48**, 1109 (1968).
[12] T. R. Hogness and H. M. Kvalnes, Phys. Rev. **32**, 942 (1928).
[13] L. G. Smith, Phys. Rev. **51**, 263 (1937).
[14] K. M. Weitzel, M. Malow, G. K. Jarvis, T. Baer, Y. Song, and Y. Ng, J. Chem. Phys. **111**, 8267 (1999).
[15] J. A. Hipple and D. P. Stevenson, Phys. Rev. **63**, 121 (1943).
[16] I. Ben-Itzhak, K. D. Carnes, S. G. Ginther, D. T. Johnson, P. J. Norris, and O. L. Weaver, Phys. Rev. A **47**, 3748 (1993).
[17] D. A. Alman and D. N. Ruzic, Phys. Plasmas **7**, 1421 (2000).
[18] R. K. Janev and D. Reiter, Forschungszentrum-Jülich Report No. 3966, 2002.
[19] R. K. Janev and D. Reiter, Phys. Plasmas **9**, 4071 (2002).
[20] HYDKIN, http://www.eirene.de/eigen/index.html
[21] A. A. Viggiano, A. Ehlerding, S. T. Arnold, and M. Larsson, J. Phys.: Conf. Ser. **4**, 191 (2005).
[22] J. B. A. Mitchell, G. Angelova, C. Rebrion-Rowe, O. Novotny, J. L. LeGarrec, H. Bluhme, K. Seiersen, A. Svendsen, and L. H. Andersen, J. Phys.: Conf. Ser. **4**, 198 (2005).
[23] M. E. Bannister, H. F. Krause, C. R. Vane, N. Djurić, D. B. Popović, M. Stepanović, G. H. Dunn, Y.-S. Chung, A. C. H. Smith, and B. Wallbank, Phys. Rev. A **68**, 042714 (2003).
[24] D. B. Popović, N. Djurić, K. Holmberg, A. Neau, and G. H. Dunn, Phys. Rev. A **64**, 052709 (2001).
[25] N. Djurić, S. Zhou, G. H. Dunn, and M. E. Bannister, Phys. Rev. A **58**, 304 (1998).
[26] N. Djurić, Y.-S. Chung, B. Wallbank, and G. H. Dunn, Phys. Rev. A **56**, 2887 (1997).
[27] J. Lecointre, H. C. Hassani, J. J. Jureta, D. S. Belić, and P. Defrance, XXIV Conference on the Physics of Electronic and Atomic Collisions—ICPEAC, Rosario, Argentina, 20–2 July 6, 2005 (unpublished); (private communication).
[28] L. Vejby-Christensen, L. H. Andersen, O. Heber, D. Kella, and

H. B. Pedersen, Astrophys. J. **483**, 531 (1997).
[29] S. G. Lias, in *NIST Chemistry WebBook, NIST Standard Reference Database Number 69*, edited by P. J. Linstrom and W. G. Mallard (National Institute of Standards and Technology, Gaithersburg MD, 2005), p. 20899 (http://webbook.nist.gov).
[30] W. Zong, G. H. Dunn, N. Djuric, M. Larsson, C. H. Greene, A. Al-Khalili, A. Neau, A. M. Derkatch, L. Vikor, W. Shi, A. Le Padellec, S. Rosen, H. Danared, and M. af Ugglas, Phys. Rev. Lett. **83**, 951 (1999).
[31] A. Le Padellec, N. Djuric, A. Al-Khalili, H. Danared, A. M. Derkatch, A. Neau, D. B. Popovic, S. Rosen, J. Semaniak, R. Thomas, M. af Ugglas, W. Zong, and M. Larsson, Phys. Rev. A **64**, 012702 (2001).
[32] N. Djuric, G. H. Dunn, A. Al-Khalili, A. M. Derkatch, A. Neau, S. Rosen, W. Shi, L. Vikor, W. Zong, M. Larsson, A. Le Padellec, H. Danared, and M. af Ugglas, Phys. Rev. A **64**, 022713 (2001).
[33] J. Lecointre, H. Cherkani, J. J. Jureta, D. S. Belić, and P. Defrance, in *Proceedings of the 22nd Symposium on Physics of Ionized Gases—SPIG*, National Park Tara, Bajna Basta, Serbia and Montenegro, 23–27 August 2004, edited by Ljupco Hadzijevski (Vinca Institute of Nuclear Sciences, Beograd, 2004), p. 63.
[34] D. H. Crandall, R. A. Phaneuf, and P. O. Taylor, Phys. Rev. A **18**, 1911 (1978).
[35] D. C. Gregory, P. F. Dittner, and D. H. Crandall, Phys. Rev. A **27**, 724 (1983).
[36] D. C. Gregory, F. W. Meyer, A. Müller, and P. Defrance, Phys. Rev. A **34**, 3657 (1986).
[37] M. E. Bannister, Phys. Rev. A **54**, 1435 (1996).
[38] E. M. Bahati, R. D. Thomas, C. R. Vane, and M. E. Bannister, J. Phys. B **38**, 1645 (2005).
[39] F. W. Meyer, in *Trapping Highly Charged Ions: Fundamentals and Applications*, edited by J. Gillaspy (Nova Science, Huntington, NY, 2001), p. 117.
[40] P. A. Taylor and G. H. Dunn, Phys. Rev. A **8**, 2304 (1973).
[41] P. A. Taylor, K. T. Dolder, W. E. Kauppila, and G. H. Dunn, Rev. Sci. Instrum. **45**, 538 (1974).
[42] C. R. Vane, E. M. Bahati, M. E. Bannister, and R. D. Thomas, Phys. Rev. A **75**, 052715 (2007).
[43] See, for example, M. F. A. Harrison, Br. J. Appl. Phys. **17**, 371 (1966).
[44] H. W. Xi, M.-B. Huang, B.-Z. Chen, and W.-Z. Li, J. Phys. Chem. A **109**, 9149 (2005).
[45] R. J. Blint, R. F. Marshall, and W. D. Watson, Astrophys. J. **206**, 627 (1976).